2 Nonstandard Linear Problems

The particular feature of the DWR method is its applicability to situations in which the underlying mathematical model lacks quantitative coercivity properties. As examples, we discuss the adaptive solution of the acoustic wave equation and the radiative transfer equation.

****

2.1 Adaptive soluton of the acoustic wave equation

We consider the acoustic wave equation

$$\begin{aligned} \partial_t^2 w - \nabla\cdot\{a\nabla w\} &= 0 \qquad \text{in } Q_T := \Omega \times I \\ w_{|t=0} = w^0, \quad \partial_t w_{|t=0} &= v^0 \qquad \text{on } \Omega \\ n\cdot a\nabla w_{|\partial\Omega} &= 0 \qquad \text{on } I \end{aligned}$$

where $\Omega \subset \mathbb{R}^d$, $d \geq 1$, and $I = (0,T)$; the elastic coefficient a may vary in space. We consider approximation by a 'velocity-displacement' formulation which is obtained by introducing a new velocity variable $v := \partial_t w$. Then, the pair $u = \{w, v\}$ satisfies the system of equations

$$\begin{aligned} \partial_t w - v &= 0 \\ \partial_t v - \nabla\cdot\{a\nabla w\} &= 0 \end{aligned}$$

with the natural solution space

$$V := [H^1(0,T;L^2(\Omega)) \cap L^2(0,T;H^1(\Omega))] \times H^1(0,T;L^2(\Omega))$$

We split the time interval $[0,T]$ into subintervals $I_n = (t_{n-1}, t_n]$,

$$0 = t_0 < ... < t_n < ... < t_N = T, \qquad k_n := t_n - t_{n-1}$$

At each time level t_n, let $V_h^n \subset V$ be appropriate finite dimensional subspaces. On each time slab $Q^n := \Omega \times I_n$, we define intermediate meshes $\bar{\mathbb{T}}_h^n$ which are composed of the mutually finest cells of the neighbouring meshes $\mathbb{T}_h^{n-1}$ and $\mathbb{T}_h^n$, and obtain a decomposition of the time slab into space-time cubes $Q_K^n = K \times I_n$, $K \in \bar{\mathbb{T}}_h^n$.

This construction is used in order to allow continuity in time of the trial functions when the meshes change with time. The discrete 'trial spaces' $V_{h,k}$ in space-time domain consist of functions that are $(d+1)$-linear on each space-time cell Q_K^n and globally *continuous* on Q_T. This prescription requires the use of 'hanging nodes' if the spatial mesh changes across a time level t_n.

The corresponding discrete 'test spaces' $W_{h,k}$ consist of functions that are constant in time on each cell Q_K^n, while they are d-linear in space and globally continuous on Ω.

On these spaces, we introduce the bilinear form

$$\begin{aligned} a(u,\varphi) \;:=\; & (\partial_t w,\xi)_{Q_T} - (v,\xi)_{Q_T} + (w(0),\xi(0)) \\ & + (\partial_t v,\psi)_{Q_T} + (a\nabla w,\nabla\psi)_{Q_T} + (v(0),\psi(0)). \end{aligned}$$

The Galerkin approximation seeks $u_h = \{w_h, v_h\} \in V_{h,k}$ satisfying

$$a(u_h,\varphi_h) = F(\varphi_)) := (v^0,\psi(0)) + (w^0,\xi(0)) \quad \forall \varphi_h = \{\psi_h,\xi_h\} \in W_{h,k}$$

This scheme is a 'Petrov-Galerkin' method. We again have Galerkin orthogonality for the error $e := \{e^w, e^v\}$:

$$a(e,\varphi_h) = 0, \quad \varphi_h \in V_{h,k}$$

This time-discretization scheme is called the 'cG(1) method' (*continuous* Galerkin method) in contrast to the dG method (*discontinuous* Galerkin method) frequently used for parabolic problems. From this scheme, we can recover the standard Crank-Nicolson scheme in time (combined with a spatial finite element method):

$$\begin{aligned} (w^n - w^{n-1},\varphi) - \tfrac{1}{2}k_n(v^n + v^{n-1},\varphi) &= 0 \\ (v^n - v^{n-1},\psi) + \tfrac{1}{2}k_n(a\nabla(w^n + w^{n-1}),\nabla\psi) &= 0 \end{aligned}$$

This system splits into two equations, a discrete Helmholtz equation and a discrete L^2-projection.

In order to embed the present situation into the general framework, we introduce the spaces

$$\hat{V} := V \oplus V_{h,k}, \quad \hat{W} := V \oplus W_{h,k}$$

We want to control the error in terms of a functional of the form

$$J(e) := (j, e^w)_{Q_T}$$

with some density function $j(x,t)$. To this end, we again use a duality argument in space-time employing the time-reversed wave equation

$$\begin{aligned} \partial_t^2 z^w - \nabla\cdot\{a\nabla z^w\} &= j \quad \text{in } Q_T \\ z^w{}_{|t=T} = 0, \quad -\partial_t z^w{}_{|t=T} &= 0 \quad \text{on } \Omega \\ n\cdot a\nabla z^w{}_{|\partial\Omega} &= 0 \quad \text{on } I \end{aligned}$$

Its solution $z = \{-\partial_t z^w, z^w\} \in \hat{W}$ satisfies the variational equation

$$a(\varphi, z) = J(\varphi) \quad \forall \varphi \in \hat{V}$$

Then, from the general results, we obtain the error identity

$$J(e) = F(z - \varphi_h) - a(w_h, z - \varphi_h)$$

for arbitrary $\varphi_h = \{\varphi_h^w, \varphi_h^v\} \in W_{h,k}$. Recalling the definition of the bilinear form $A(\cdot,\cdot)$, we obtain the following error identity:

$$\begin{aligned} |(j,w)_{Q_T}| \le \sum_{n=1}^{N} \sum_{K\in\mathbb{T}_h^n} \big| &(R^u(u_h), \partial_t z^w - \varphi_h^v)_{K\times I_n} \\ &- (R^v(u_h), z^w - \varphi_h^w)_{K\times I_n} - (r(u_h), z^w - \varphi_h^w)_{\partial K\times I_n}\big| \end{aligned}$$

with the cell residuals

$$R^w(u_h)_{|K} := \partial_t w_h - v_h, \qquad R^v(u_h)_{|K} := \partial_t v_h - \nabla\cdot\{a\nabla w_h\}$$

and the edge residuals

$$r(w_h)_{|\Gamma\times I_m} := \begin{cases} \frac{1}{2} n \cdot [a\nabla w_h], & \text{if } \Gamma \subset \partial K \backslash \partial\Omega \\ 0, & \text{if } \Gamma \subset \partial\Omega \end{cases}$$

Numerical test (W. Bangerth 1998)

The energy-norm-type error estimator

$$\eta_E(u_h) := \Big(\sum_{n=1}^{N} \sum_{K\in\mathbb{T}_h^n} \rho_K^{n,1}(u_h)^2 \Big)^{1/2}$$

$$\rho_K^{n,1} := \|R(u_h)\|_{K\times I_n} + h_K^{-1/2} \|r(u_h)\|_{\partial K\times I_n}$$

measures the spatial smoothness of the computed solution w_h.

We consider the propagation of an outward travelling wave on $\Omega = (-1,1)^2$ with a strongly heterogeneous coefficient. Boundary and initial conditions are chosen as follows:

$$n\cdot\{a\nabla u\} = 0 \quad \text{on } y=1, \qquad w=0 \quad \text{on } \partial\Omega\backslash\{y=1\}$$

$$w_0 = 0 \quad v_0 = \theta(s-r)\exp\left(-|x|^2/s^2\right)\left(1-|x|^2/s^2\right)$$

with $s=0.02$ and $\theta(\cdot)$ the jump function. The lowest frequency in the initial wave field has wavelength $\lambda = 4s$; hence taking the usual minimum ten grid points per wavelength would yield 62 500 cells for the largest wavelength. If this example is taken as a model of propagation of seismic waves in a faulted region of rock, then the seismograms at the surface, the top line Γ of the domain, are to be recorded. A corresponding functional output is

$$J(w) = \int_0^T \int_\Gamma w(x,t)\ \omega(\xi,t)\,\mathrm{d}\xi\,\mathrm{d}t$$

with a weight $\omega(\xi,t) = \sin(3\pi\xi)\sin(5\pi t/T)$, and end-time $T=2$. The frequency of oscillation of this weight is chosen to match the frequencies in the wave field to obtain good resolution of changes.

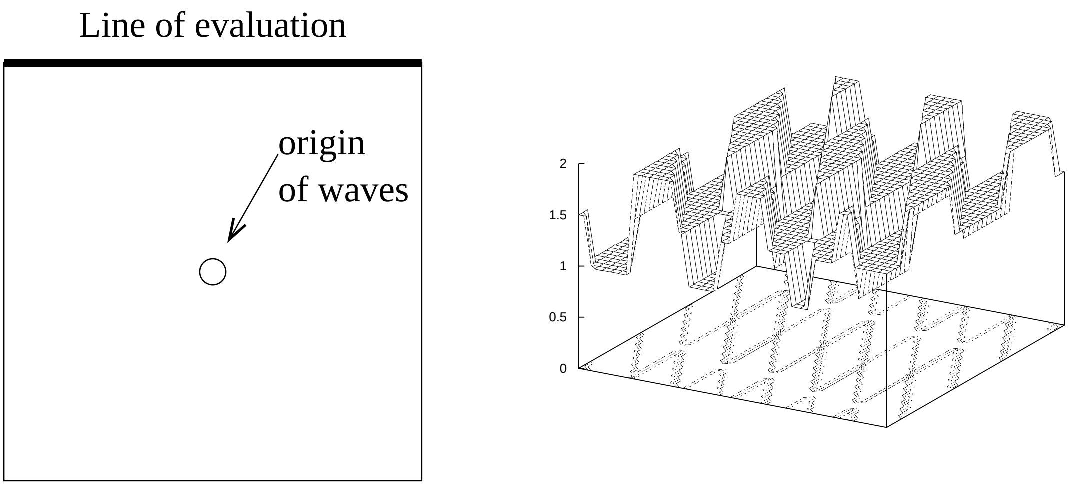

Figure. Layout of the domain (left) and structure of the coefficient $a(x)$ (right).

weighted estimator		heuristic indicator	
$N\times M$	$J(w_h)$	$N\times M$	$J(w_h)$
327 789	-2.085e-6	327 789	-2.085e-6
920 380	-4.630e-6	920 380	-4.630e-6
2 403 759	-4.286e-6	2 403 759	-4.286e-6
1 918 696	-4.177e-6	5 640 223	-4.385e-6
2 975 119	-4.438e-6	10 189 837	-4.463e-6
6 203 497	-4.524e-6	17 912 981	-4.521e-6
		41 991 779	-4.517e-6

Table. Results obtained by adaptation by the DWR method (reference value $J(w) \approx$ -4.515e-6, $M = \#$ time-steps, $N = \#$ mesh-cells.)

Remark. The evaluation of the *a posteriori* error estimate requires a careful approximation of the adjoint solution z. Therefore, a higher-order method (bi-quadratic elements) is used for solving the space-time adjoint problem.

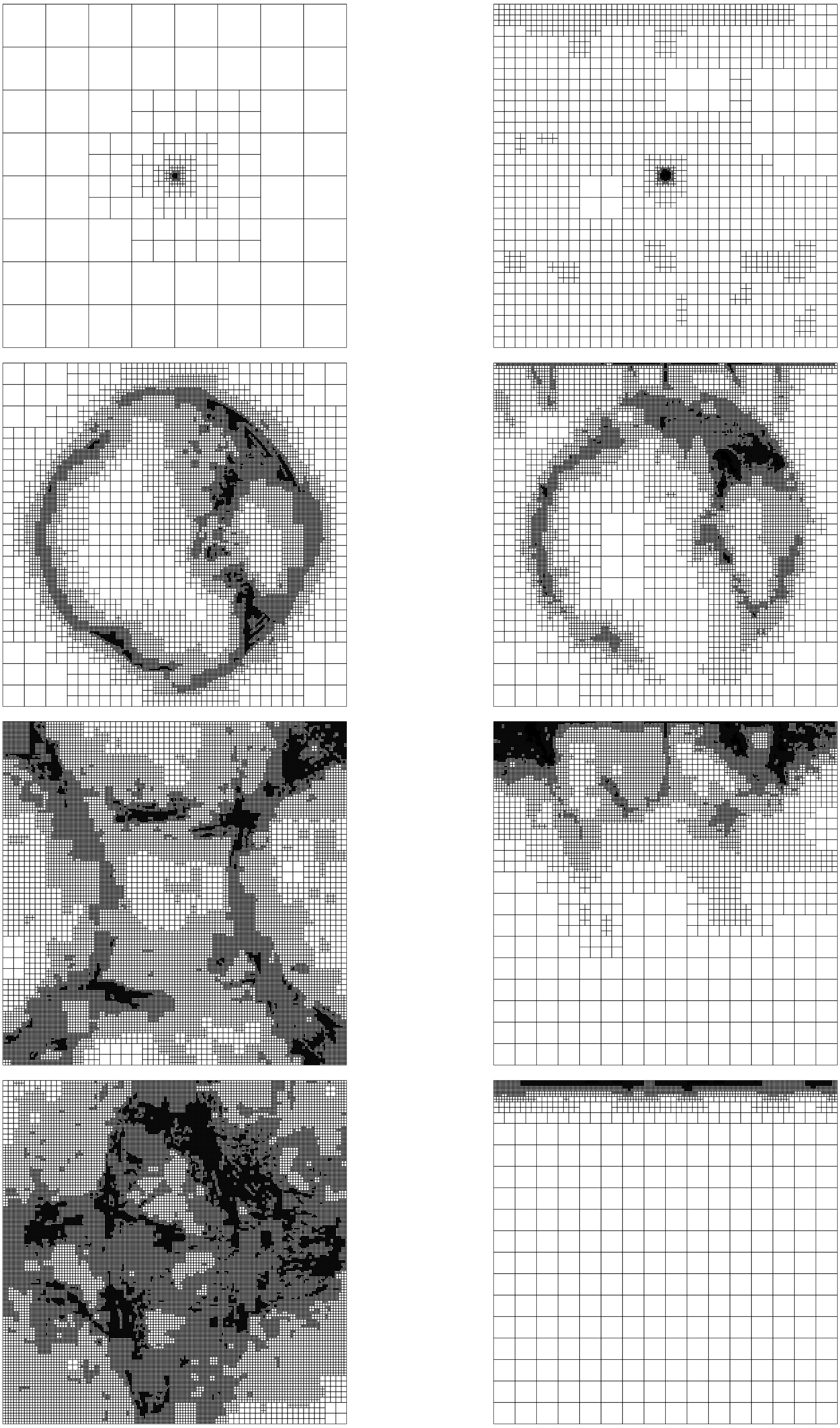

Figure. Grids produced by the energy-error indicator (left) and by the weighted estimator (right), at times $t = 0,\ \frac{2}{3},\ \frac{4}{3},\ 2$.

2.2 Application to radiative transfer

Radiative transfer equation for intensity $u = u(x, \theta, \lambda_*)$

$$\theta \cdot \nabla_x u + (\kappa + \mu) u = \mu \int_{S_2} k(\theta, \theta') u \, d\theta' + B \quad \text{in } \Omega \times S_2,$$

$$u = 0 \quad \text{auf } \Gamma_{\text{in},\theta} = \{x \in \partial\Omega, \, n \cdot \theta \le 0\}.$$

Given: Absorption κ, scattering μ, recombination $k(\cdot,\cdot)$,
radiation source (Planck function) B.

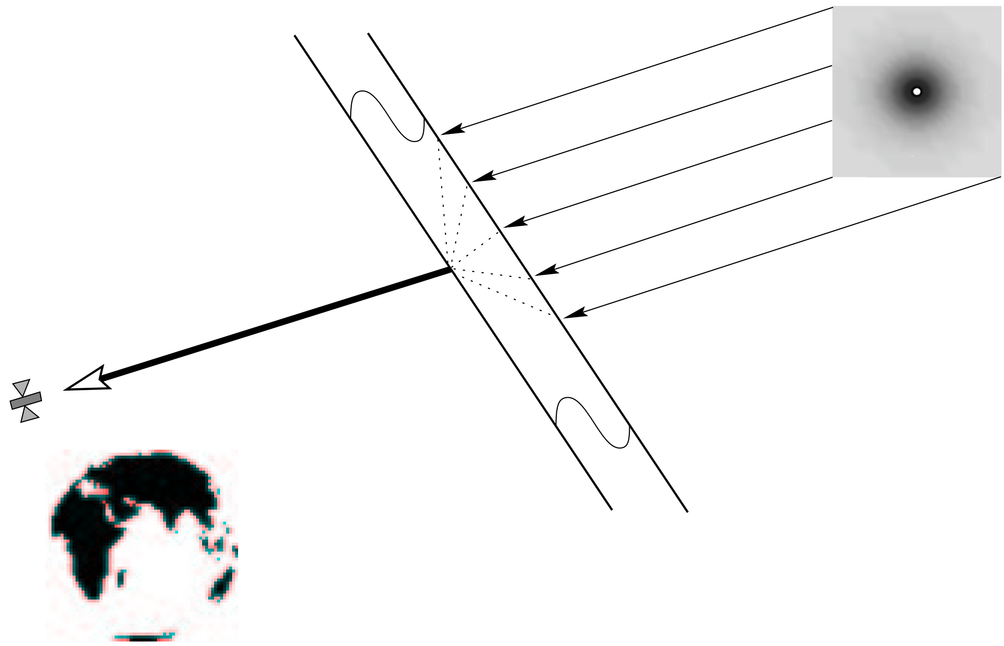

Computation of observed mean intensity

$$J(u) = \int_{\{n \cdot \theta_{\text{obs}} \ge 0\}} u(x, \theta_{\text{obs}}) \, ds, .$$

Finite element Galerkin discretizierung with $V_h \subset H^1(\Omega) \times L^2(\Omega)$

$$((T + \Sigma) u_h, \varphi_h)_{\Omega \times S_2} = (B, \varphi_h)_{\Omega \times S_2} \quad \forall \varphi_h \in V_h,$$

$$T u_h := \theta \cdot \nabla_x u_h, \quad \Sigma u_h := (\kappa + \mu) u_h - \mu \int_{S_2} K(\theta, \theta') u_h \, d\theta'.$$

Numerical test (G. Kanschat 1996):

	L^2 indicator		weighted indicator			
L	N_x	$J(u_h)$	N_x	$J(u_h)$	η_ω	$\eta_\omega/J(e)$
1	564	0.181	576	0.417	3.1695	23.77
2	1105	0.210	1146	0.429	1.0804	8.62
3	2169	0.311	2264	0.461	0.7398	7.11
4	4329	0.405	4506	0.508	0.2861	3.94
5	8582	0.460	**9018**	**0.555**	0.1375	3.33
6	17202	0.488	18857	0.584	0.0526	2.39
7	34562	0.537	39571	0.599	0.0211	1.76
8	**68066**	**0.551**	82494	0.608	0.0084	1.41
			∞	0.618		

Table. Adaptive solution of the radiative transfer equation with a (heuristical) L^2-error indicator and the weighted error indicator; total number of degrees of freedom: $N_{\text{tot}} = N_x \cdot 32$

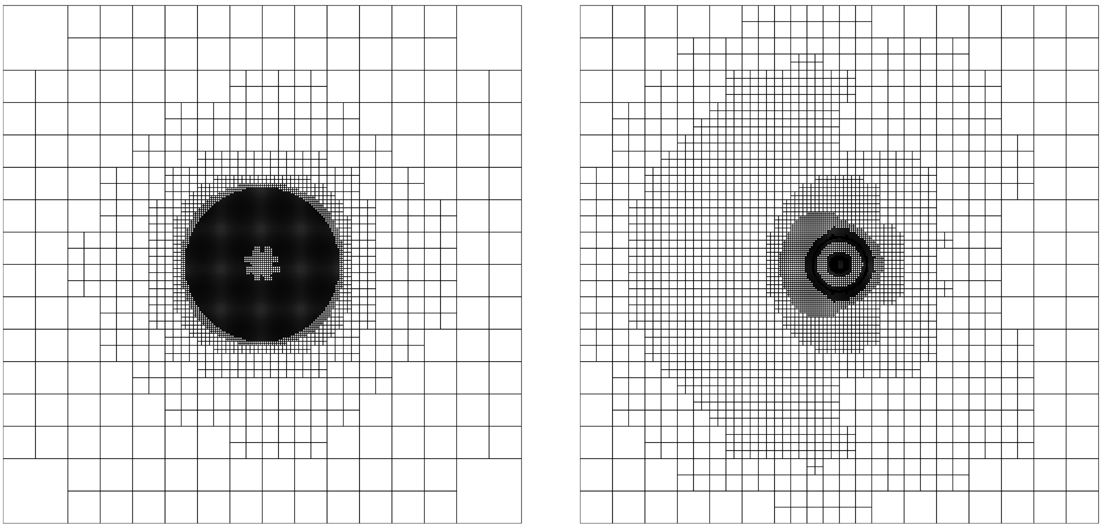

Figure. Adapted meshes obtained by the L^2-error indicator (left) and by the weighted error indicator (right)